Geoscience Frontiers 15 (2024) 101730

Contents lists available at ScienceDirect

Geoscience Frontiers

journal homepage: www.elsevier.com/locate/gsf

Research Paper

Factor analysis of recent major heatwaves in East Asia

Arim Yoon [a], Jeongwon Kim [a], Jooyeop Lee [a], Hyun Min Sung [b], Je-Woo Hong [c], Seung-Ki Min [d,f], Junhong Lee [e], Jinkyu Hong [a,*]

[a] Ecosystem-Atmosphere Process Laboratory, Department of Atmospheric Sciences, Yonsei University, Seoul 03722, Republic of Korea
[b] National Institute of Meteorological Sciences, Jeju 63568, Republic of Korea
[c] Korea Adaptation Center for Climate, Korea Environment Institute, Sejong 30121, Republic of Korea
[d] Division of Environmental Science and Engineering, Pohang University of Science and Technology, Pohang 37673, Republic of Korea
[e] Max Planck Institute for Meteorology, Hamburg 20146, Germany
[f] Institute for Convergence Research and Education in Advanced Technology, Yonsei University, Seoul, South Korea

ARTICLE INFO

Article history:
Received 4 March 2023
Revised 20 August 2023
Accepted 13 October 2023
Available online 18 October 2023
Handling Editor: Sanghoon Kwon

Keywords:
Heatwave
East Asia
Large-scale circulation
Soil moisture
Sea surface temperature
Synergistic impacts

ABSTRACT

Heatwaves (HWs) present a major hazard to our society and more extreme heatwaves are expected with future climatic changes. Hence, it is important to improve our understanding of the underlying processes that drive HWs, in order to boost our socioeconomic–ecological resilience. In this study, we quantified the influences of key driving factors (large-scale atmospheric circulation, soil moisture, and sea surface temperature) and their synergies on recent heatwaves in East Asia. We conducted a factor separation analysis for three recent HW events by constraining the key factors in the regional Weather Research and Forecasting model with their climatologies or pseudo-observations in different combinations. Our study showed distinct spatial variations in the HW-controlling factors in East Asia. The synergistic interaction of large-scale circulation and soil moisture was the most important factors in the 2013 Chinese HW. During the 2018 HWs in Korea and Japan, the same stagnant large-scale atmospheric circulation played a dominant role in driving the HW events. The land-atmosphere coupling via soil moisture, its interaction with circulation, and SST exhibited stronger influences during the Korean HW than the Japanese HW. Our analysis also revealed temporal variations in the factors driving Korean and Chinese HWs due to typhoon passage and other multiple processes over heterogeneous surfaces (i.e., topographically induced Foehn winds, large-scale warm advection from the warm ocean, spatial differences in soil moisture). Our findings suggest that future heatwave-related studies should consider interactive contributions of key factors, their interplay with surface heterogeneities of complex terrain.

1. Introduction

Heatwaves (HWs) present an increasing risk to society because of their potential to threaten socio-ecological sustainability (e.g., health, food, and water security). Drastic increases in the frequency, intensity, and persistence of HWs have been reported worldwide (e.g., Meehl and Tebaldi, 2004; Perkins et al., 2012; Lin et al., 2022; Neal et al., 2022; Dong et al., 2023). Particularly, unprecedented HWs have occurred worldwide in the last decade (e.g., Australia in 2018, Europe in 2019 and 2022, North America in 2021, Siberia HW in 2020, and East Asia in 2022). This increase in extreme temperature events demands an improved understanding of heatwave drivers and underlying physical processes. Such understanding is vital to facilitate sustainable development and inform climate change adaptation policies to mitigate HW damage.

Atmospheric modeling studies have provided useful insights on heatwave generation and reinforcement (e.g., Black et al., 2004; Cassou et al., 2005; Seneviratne et al., 2013; Wehrli et al., 2019). By controlling the factors driving the HWs with a series of sensitivity experiments, these modeling studies have resulted in substantial progress in identification of driving processes of HWs. Established driving factors include large-scale atmospheric circulation (CIR) by persistent anticyclonic systems and the related heat accumulation due to reduced cloud cover (e.g., Nakamura and Fukamachi, 2004; Sui et al., 2007; Ding et al., 2010; Dole et al., 2011; Pfahl and Wernli, 2012; Yoon et al., 2020; Choi et al., 2022), soil moisture (SM) (e.g., Seneviratne et al., 2006, 2010; Hirschi et al., 2011; Hauser et al., 2016), sea surface temperature (SST) (e.g., Black et al., 2004; Cassou et al., 2005; Petch et al., 2020),

* Corresponding author.
E-mail address: jhong@yonsei.ac.kr (J. Hong).

https://doi.org/10.1016/j.gsf.2023.101730

and topographically induced local wind patterns and urban heat islands (e.g., Ma et al., 2014; Chen and Lu, 2015; Yoon et al., 2018; Hong et al., 2019).

Importantly, these driving factors also interact with each other, leading to varied HWs. For example, if HW is generated over dry soil, HW intensity is then more likely to increase because of more partitioning of surface energy into direct heat transfer into the atmosphere (i.e., decrease in evaporative fraction (*EF*) defined as the fraction of latent heat fluxes to surface net radiation) with increased atmospheric water demand. Indeed, these land–atmosphere coupling intensified HWs under stagnant CIR through the reduction of SM and the related decrease in *EF* (Seneviratne et al., 2006; Fischer et al., 2007; Lorenz et al., 2010; Hirschi et al., 2011; Miralles et al., 2014). This SM–temperature feedback fosters HW-favorable conditions and typically occurs over transitional climate zones between arid and humid zones (Koster et al., 2004; Seneviratne et al., 2006; Jiang et al., 2023). Warm SST also drives HW occurrence upon interaction of SST with stagnant CIR. This is because intense HW can lead to an increase in air temperature by releasing the heat stored in the upper ocean layer into the atmosphere and by warm air advection inland (Frölicher and Laufkötter, 2018; Yeh et al., 2018; Petch et al., 2020; Wie et al., 2021).

Key feedback processes of HW generation and reinforcement show spatio-temporal variation with changes in feedback strength and weather conditions. For example, recent European HWs were driven by SM reduction in 2003 and 2010 (Fischer et al., 2007; Teuling et al., 2010; Dole et al., 2011; van Garderen et al., 2021), by CIR patterns in 2015 (Duchez et al., 2016; Wehrli et al., 2019; Rousi et al., 2022) but not by SST (Dole et al., 2011; Hauser et al., 2016). African HWs in 2016 were related to high-pressure anomalies and droughts induced by strong El Niño events (e.g., Iskandar et al., 2018; Yuan et al., 2018; Wehrli et al., 2019). By performing a series of global climate model simulations that used climatological averages and observations of HW driving factors, Wehrli et al. (2019) quantified the relative contributions of factors driving recent HWs across different continents. Despite several studies that consider the mechanisms that generate HWs, more research is needed that considers the interaction between HW driving mechanisms, and spatio-temporal variations in the physical mechanisms at regional scales.

East Asia is vulnerable to HWs because of its highly populated megacities that have exhibited rapid economic growth since the 1980s. Because of the potentially disastrous socioeconomic impacts of HWs in East Asia on food and water scarcity, it is necessary to understand the physical mechanisms and relative contributions of factors driving extreme HWs. East Asia is climatologically in a transitional climate zone. The land–atmosphere coupling is strong, and evapotranspiration is therefore sensitive to SM (Koster et al., 2006; Zhang et al., 2011; Zscheischler and Seneviratne, 2017). Furthermore, East Asia is located adjacent to the Pacific Ocean and in the eastern boundary region of the Eurasian continent, so it is expected that complex physical processes are involved in HW generation. However, low-resolution global atmospheric models are limited in their application to studying HW driving mechanisms in this critical region. Their limitations arise from the region's small-scale surface heterogeneity due to complex land use, land cover, and the topography (i.e., mountains through to oceans). Recent studies suggested a single dominant factor by the coupling of the atmosphere with soil moisture or the anti-blocking of the large-scale pressure system in the Chinese continent rather than by combination of various factors and feedback processes (e.g., Ha et al., 2020; Seo and Ha, 2022; Jiang et al., 2023).

The objectives of this study are to examine the role of SM, SST, and CIR as factors influencing recent HWs and their spatial and temporal variations in East Asia. In this study, we used the Alpert–Stein factor separation methodology for the high-resolution atmospheric model (Stein and Alpert, 1993), Weather Research and Forecasting (WRF) model to identify underlying processes of major recent HWs over complex terrain at regional scales in East Asia. Particularly, our study quantifies the synergetic interactions of driving factors and sensitivity of HWs to critical variables.

2. Materials and methods

2.1. Heatwave events

Our study investigated three recent extreme HW events in East Asia (Fig. 1). HWs in these regions was determined by the 90th percentile of the climatological TX as a threshold during summer season for the period of 1981–2009 (Perkins et al., 2012; Yoon et al., 2020; Kawase et al., 2020). That is, heatwave events in these regions were defined if the daily maximum air temperature (TX) exceeded top 10% of TX for 1981–2009 for a given day of the year for more than three days (Fig. 2). The mean TX anomaly from its climatology for HWs in China was 5.1 °C during the HW period, which was the hottest summer in 141 years before 2022 (Yuan et al., 2016). The HW persisted in eastern China near the Yangtze River valley for two weeks from August 5, 2013, and was terminated by two typhoons. SM showed negative anomalies in southern China (Fig. 3a). The percentage of averaged SM anomaly during the HWs reached nearly −50% (with a z-score of −1.92), with particularly dry regions found around the Yangtze River valley.

HW cases were also reported in South Korea and southern Japan in 2018, both of which were record-breaking HW events in their respective countries (Korea Meteorological Administration; KMA, 2018; Japan Meteorological Agency; Jma, 2018). The 2018 Korean HW persisted for 25 days (from July 12 to August 5) with a mean TX anomaly of 5.4 °C (Fig. 2b). The 2018 Japanese HW persisted for 11 days (from July 14 to July 25), with a TX anomaly of 4.9 °C (Fig. 2c). There was a spatial gradient of SM between the western and eastern Korean Peninsula (Fig. 3b). SM anomalies were smaller, with −30% SM anomalies (z-score of −1.44) on the western side of the peninsula. In Japan, SM anomalies were uniformly distributed at −10% (z-score of −0.5) (Fig. 3c).

2.2. Model design

We used the regional climate model, WRF. The horizontal resolution over East Asia (24°N–46°N, 108°E–142°E; Lambert conformal map) is 25 km and the vertical layer consisted of 31 levels up to 50 hPa. The physical packages of the simulation were the same as those used by Lee et al. (2020) and the references therein (Supplementary Data, Table S1). Initial and boundary conditions are from 6-hourly European Centre for Medium-Range Weather Forecasts reanalysis version 5 (ERA5) data (Hersbach et al., 2020). The WRF model reproduced both the magnitude of TX and its spatio-temporal variations in air temperature when compared to ERA5 in the real simulation (i.e., ALL experiment in Supplementary Data, Table S1). There were underestimations in air temperature owing to relatively ample initial soil moisture than that in ERA5, which has the potential to influence our results even though factor analysis relies on differences between the various model experiments (Supplementary Data, Fig. S1).

Factor analysis was performed by constraining model boundary conditions with different combinations of climatological and observational values, similar to previous modeling studies (e.g., Wehrli et al., 2019). The factor separation method has been used to investigate the effects of atmospheric variables and surface

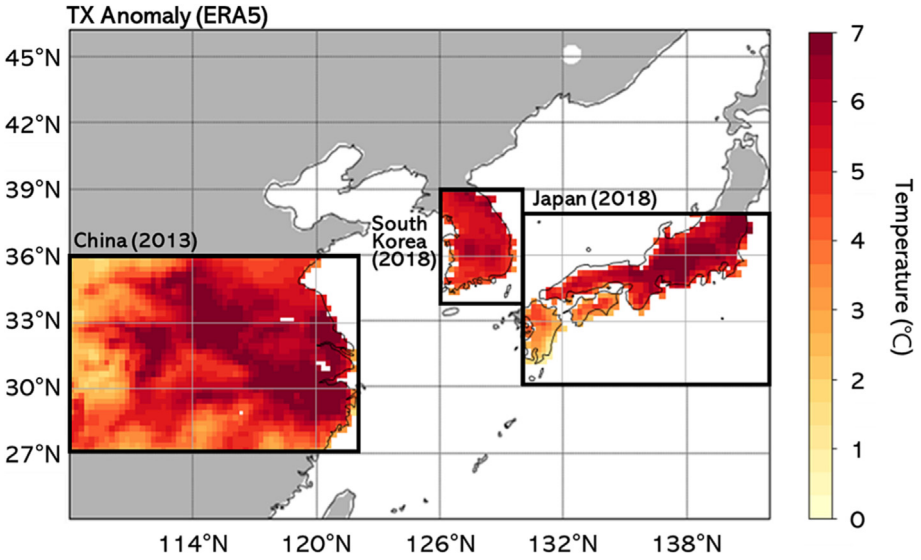

Fig. 1. Domain configuration for the WRF simulation with the ERA5 daily maximum temperature (TX) anomaly map for the study regions (HWs in China in 2013, South Korea in 2018, and Japan in 2018).

types on target processes, considering factors both individually and in their combination (e.g., Stein and Alpert, 1993; Goyette, 2017). Factor analysis does not give causality information but is an effective way to quantify the relative contribution of each factor and factor combinations by conducting a series of sensitivity simulations when it is combined with physical interpretation (Stein and Alpert, 1993). This study applied Alpert–Stein factor analysis to quantify the impacts of three key influential factors on HW generation and intensity (i.e., CIR, SM, and SST) with their related feedback processes reported in previous studies. In this study, we performed eight sensitivity simulations to elucidate the key HW driving factors by prescribing their climatological averages (1981–2009) or pseudo-observations during the HW days to the model outputs (Supplementary Data, Table S2). The contribution of each factor was estimated by subtracting the simulated TX between the sensitivity experiments. The interaction among multiple factors was calculated as a combination of several simulations (Supplementary Data, Table S3). All values were normalized by their total anomalies and expressed as percentages of their relative contributions to the respective TX anomaly.

There is the lack of realistic high-resolution SM observations for the model validation and pseudo-observations of SM from reanalysis data and offline land surface model (LSM) have been used for the LSM consistency in the soil moisture related studies (e.g., Lim et al., 2012; van den Hurk et al., 2012). Pseudo-observation of SM is discussed at by Gómez et al. (2020) in more detail. In this study, high-resolution pseudo-observational and climatological SM values were generated to isolate the SM impact on HW using High-Resolution Land Data Assimilation (HRLDAS, version 3.7.1), driven by ERA5 atmospheric data with a 4-year spin-up time in East Asia based on Lim et al. (2012). The spin-up SM was relatively smaller than that of ERA5, which contributed to cooler air temperature simulated by the WRF (not shown here).

Atmospheric nudging is an effective way to constrain large-scale features in the regional model (e.g., Song et al., 2018; van Garderen et al., 2021). In this study, the nudging was applied every 6 h to impose the CIR in ERA5 above 700 hPa, so that atmospheric boundary layer evolves freely, similar to the approach taken by Wehrli et al. (2018). SST was prescribed every 24 h considering the time-varying SST data from the ERA5 over the entire model domain. The effect of the time lag between SST and air temperature was imposed on the model simulations because all weather conditions (including temperature) were simulated in the model simultaneously with these prescribed realistic and climatological SSTs.

3. Results

3.1. The 2013 Chinese heat wave

Previous studies have reported the western North Pacific subtropical high (WNPSH) (Wang et al., 2018), SST (Li et al., 2015), and SM (Jiang et al., 2023) as the main factors driving recent HWs in southern China. Our results indicate that the impact of CIR, SM, and CIR–SM synergy were crucial in generation and reinforcement of the 2013 Chinese HW, and that SST was not a key feedback factor in this HW event (Fig. 4). Despite the strong spatial correlation of TX with SM over southern China, we found that SM alone did not lead to substantial HW occurrence (i.e., C_{SM} is not the dominant factor). The singular impacts of SM (C_{SM}) and CIR (C_{CIR}) on the HW resulted in 31% and 22% of the total observed TX anomaly, respectively. Notably, the interaction between CIR and SM (I_{CIR_SM}), which has not been quantified in previous studies, played a dominant role in this HW event, explaining 44% of the TX anomaly. Other synergistic effects had minor effects on the 2013 Chinese HW (Fig. 4).

Strong and stable anticyclonic anomalies were observed over southeastern China during the HW period in all the experiments where observed CIR patterns were imposed in the model (e.g., Fig. 5a). The WNPSH abnormally extended its system further west and persisted over eastern China during the HW period. The pseudo-CIR-prescribed experiments (i.e., E_CIR, E_CIR-SM) revealed that persistent subsidence by the WNPSH system led to a large amount of surface shortwave radiation and decreased precipitation, providing a favorable environment for heating (Supplementary Data, Fig. S2a).

Drought and associated low SM before the HW event were also important factors. The summer monsoon ended on June 28, 2013, which was earlier than the annual norm. China experienced severe drought with low precipitation and humidity, particularly along the Yangtze River (Fig. 3) (Yuan et al., 2016). A reduction in SM and a consequent decrease in *EF* (i.e., increase in sensible heat flux)

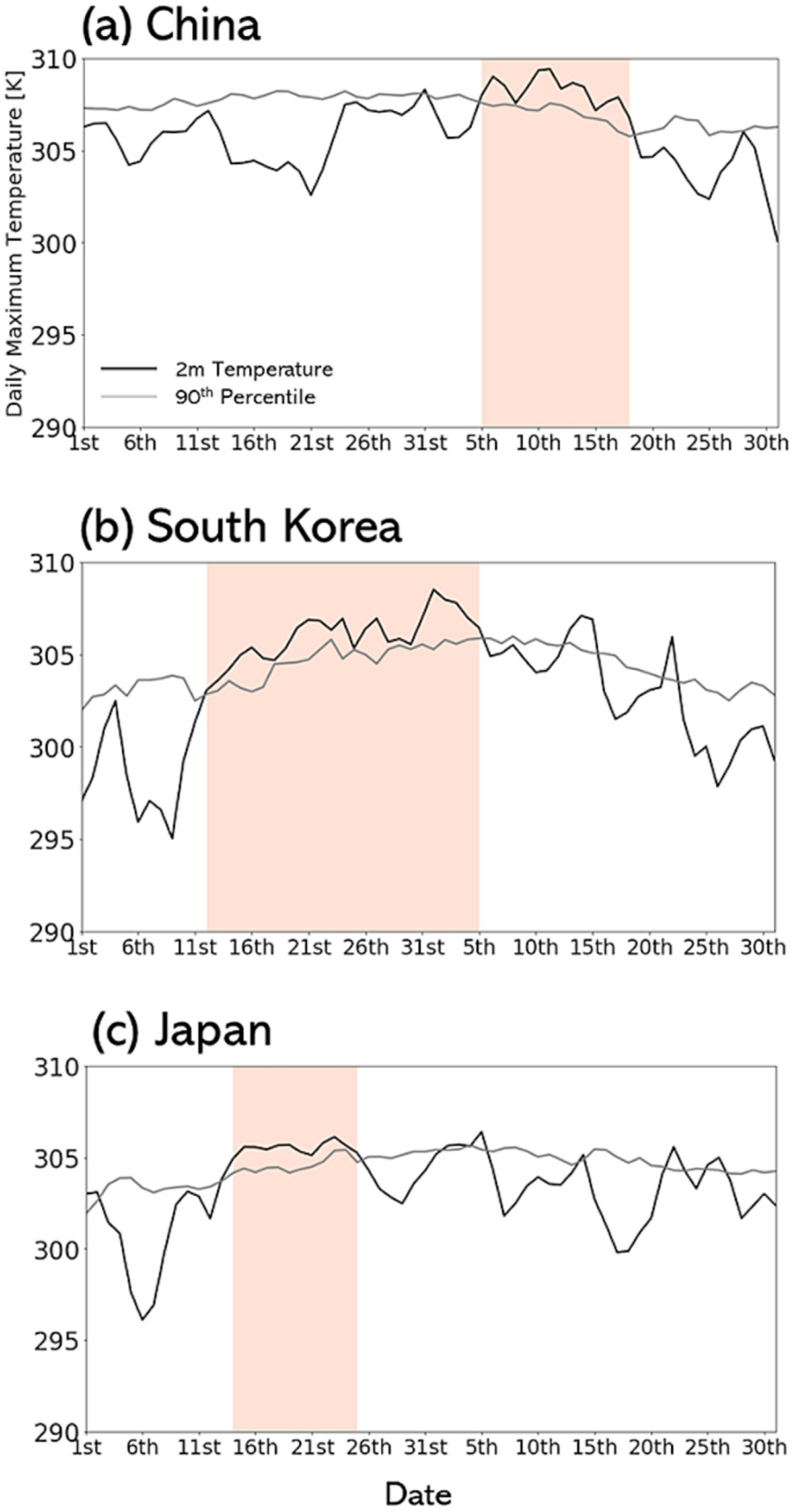

Fig. 2. Time series of TX using ERA5 2 m temperature data (black line) with the 90th percentile (gray line) from the last three decades for (a) China, (b) South Korea, and (c) Japan. The periods highlighted in color correspond to the HW events considered in this study and indicate where the TX exceeded the climatological thresholds for at least three consecutive days.

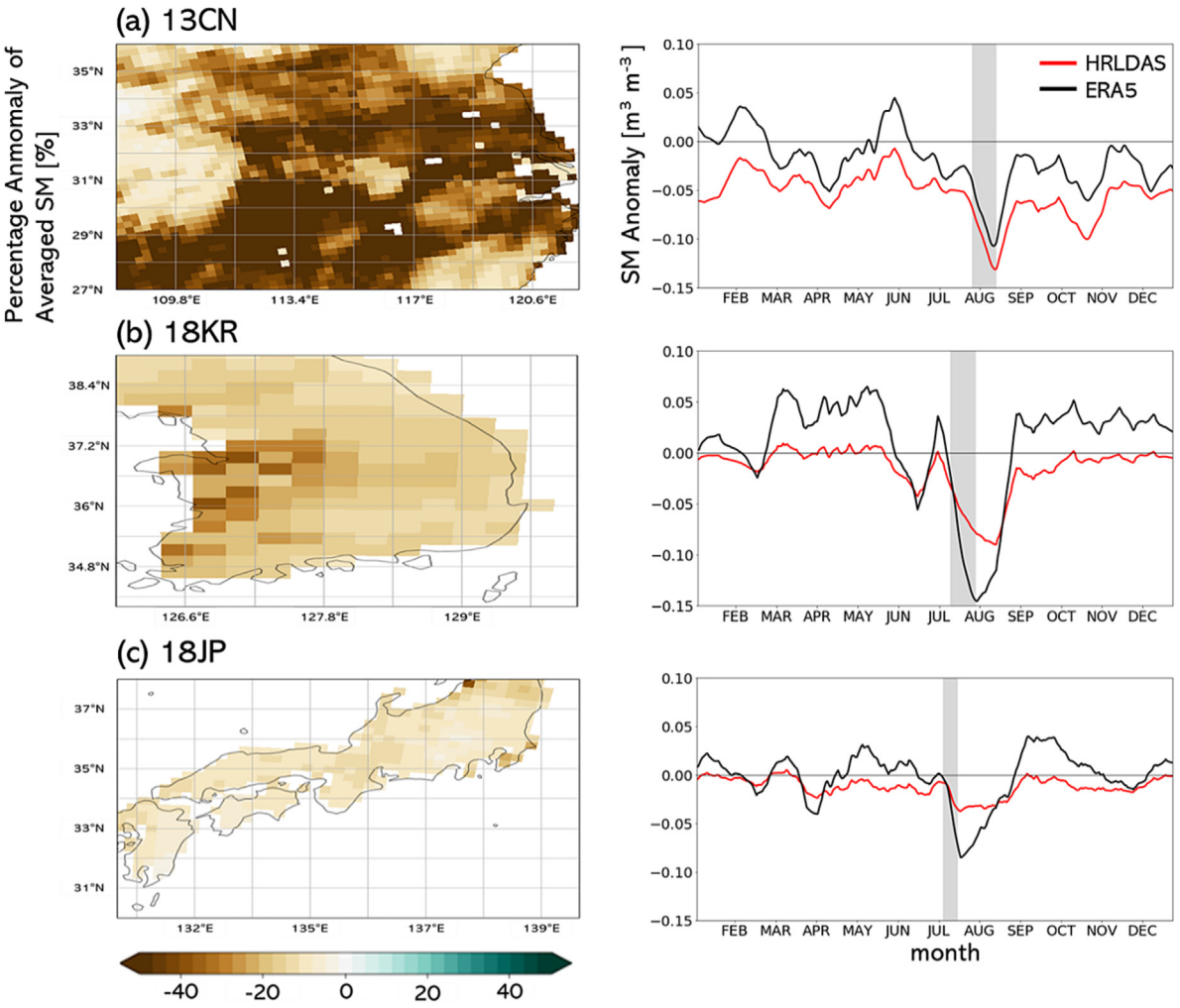

Fig. 3. Spatial distribution of SM anomaly (deviation from the climatological values for 1981–2009) for the considered HWs in (a) China, (b) Korea, and (c) Japan. SM anomaly given as a percentage from HRLDAS (left panel) and as a time series of yearly SM anomaly changes for each HW region from HRLDAS (10 cm depth, coral line) and ERA5 (7 cm depth, olive line) (right panel). The HW periods are highlighted in gray.

were apparent in the model, especially when pseudo-observational SM was prescribed (Supplementary Data, Fig. S2b). This is similar to results reported in previous studies in Europe, North America, and East Asia (e.g., Betts et al., 1996; Seneviratne et al., 2006; Miralles et al., 2019; Benson and Dirmeyer, 2021; Jiang et al., 2023). Our results also showed that this moisture–temperature coupling was critical in the transitional climate zones around the Yangtze River valley. Our findings added that it was specifically the combination of factors responsible for the HW generation, and not the single factors alone.

With seasonal march of the CIR pattern, there were temporal changes in the effect of CIR alone, as well as the synergistic effect of CIR and SM (Fig. 6a and b). Notably, the TX anomaly varied according to changes in CIR contribution. Under the stagnant high pressure, a HW-favorable conditions were provided by significant shortwave radiation reaching the surface (Supplementary Data, Fig. S2). This process led to an increase in sensible heat and the atmospheric water demand, resulting in continuous declines of soil moisture. This mechanism was also confirmed in our study through Evaporative Fraction (*EF*), indicating decreases in soil moisture during the entire HW period (Supplementary Data, Fig. S3b and Fig. S4a). During the mid-HW period of the maximum TX anomalies, CIR, SM and CIR-SM contributions increased, but the relative contribution of SM decreased because of more increases in the CIR and CIR-SM effects. During the driest soil moisture period in the late HW period, SM and CIR-SM contributions tended to decrease because the weaken stagnant circulation by the effects of typhoons and subsequent decreases in surface radiation (Supplementary Data, Fig. S2). This indicates that temporal changes in the WNPSH are critical for shaping the temporal evolution of HW events in this region.

3.2. The 2018 Korean heat wave

Previous research has reported that persistent anticyclones over the Korean Peninsula were the main factors controlling the 2018 HW (Liu et al., 2019; Shimpo et al., 2019; Ha et al., 2020; Ren et al., 2020). CIR was the dominant factor in the 2018 Korean HW, with a 65% contribution to the TX anomaly (Fig. 4) and stagnant high-pressure blocking caused heat accumulation near the surface by anomalously high downward shortwave radiation which was similar to the HW generation mechanism reported in previous studies (Fig. 5b and Supplementary Data, Fig. S2c).

Singular impacts of SM (C_{SM}) and SST (C_{SST}) on the HW explained approximately 15% of the total TX anomaly, respectively. SST had a relatively larger impact than for the 2013 Chinese HW, with a relatively higher SST around the Korean Peninsula (Supplementary Data, Fig. S5). SST increased monotonically during the

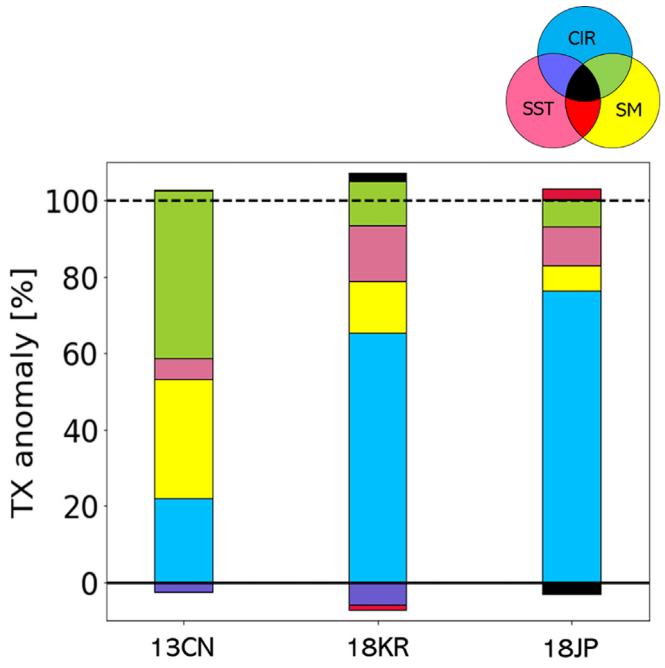

Fig. 4. Relative contributions (in %) of the physical factors driving the TX anomaly for the studied HW events. All values are averaged over the entire spatial domains shown in Fig. 1. Each factor's contribution is normalized by the simulated total TX anomaly (ALL – CTL). Colors in the Venn diagram indicate contributions of singular factors and the interaction of multiple factors.

heatwave events and its correlation of TX was larger than 0.8 (not shown here) but not a dominant factor for the HW. The combination of SST and CIR (i.e., negative I_{CIR_SST}) reduced the total influence of SST, suggesting that there is an interactive process to reduce warm SST impact on HW in this region which needs to be investigated in future research. The contribution from the CIR–SM interaction (I_{CIR_SM}) was not as significant as in the 2013 Chinese HW, possibly because of relatively ample soil moisture just before the onset of the Korean HW event (i.e., SM memory effect).

Our findings also showed a significant temporal variability in the dominant factor during the 2018 Korean HWs, particularly in the CIR and SM contributions (Fig. 6c and d). The anomalous high WNPSH was the dominant factor that contributed to the onset of the HW, and C_{CIR} maintained its strength until July 29th. This CIR influence decreased as the SST influence increased gradually from July 25th to 31st, when the Korean Peninsula was indirectly affected by Typhoon Jongdari. The typhoon moved around the southern edge of the strong high-pressure zone located over the northern Korean Peninsula (Fig. 5b). However, the typhoon caused substantial changes in the large-scale pressure pattern across East Asia; hence, the CIR effects tended to decrease following the typhoon, with decreases in the absolute magnitude of TX (Fig. 6c and d). However, the absolute contribution of other drivers did not change significantly compared to the CIR effect during the typhoon passage (i.e., decoupling from the typhoon), and consequently their relative contribution increased substantially because of the lower impact of the CIR after the typhoon passage (Fig. 6d).

Wind direction changed from southwesterly to easterly after the typhoon passage. The easterly wind enhanced large-scale warm advection from the warm ocean to the Korean Peninsula, leading to an increase in air temperature (Supplementary Data, Figs. S2 and S3). The easterly wind produced temperature increases over western Korea located on the lee side of the Taebaek Mountains which extends in the north–south direction along the eastern coast of the Korean Peninsula (Fig. 7). The 2018 HW in this region has been reported as the Foehn effect by topography in previous studies on this HW event (e.g., KMA, 2018; Wie et al., 2021). Accordingly, the wind direction change contributed to the enlarged contribution of the CIR–SST interaction; this effect decreased as the easterly wind disappeared with the anticyclone re-stretching over the peninsula (Fig. 6d).

We also speculate that dry and warm air from the easterly wind reinforced the interaction between CIR and low SM conditions by increasing the atmospheric demand for water and subsequent evapotranspiration (Supplementary Data, Fig. S6). Indeed, there were subsequent increases in the contribution of SM to the TX anomaly after the typhoon passage (Fig. 6d). SM was comparable to its climatology before the beginning of the HW (Fig. 3b), and the singular SM effect was negligible in the early HW periods (Fig. 6c and d). There was a 20% – 30% contribution of the SM–CIR interaction before the typhoon passage. As SM gradually decreased with the ongoing HW (Fig. 3b), the SM anomaly changed from positive to negative (Fig. 3b) and contributed to the increasing temperature throughout the entire HW period (Fig. 6c and d).

3.3. 2018 Japanese heat wave

The singular CIR was a dominant factor in the 2018 Japanese HW, explaining 76% of the total TX anomaly (Fig. 4). This CIR contribution was greater than that in the Korean and Chinese HWs. Spatio-temporal variations in TX were well correlated with the singular contribution of CIR (Fig. 6e), similar to the 2018 Korean HW. Previous studies also reported that 2018 HWs in East Asia were primarily caused by the large-scale WNPSH (e.g., Shimpo et al., 2019). Similar to the 2018 Korean HW, most of Japan was under

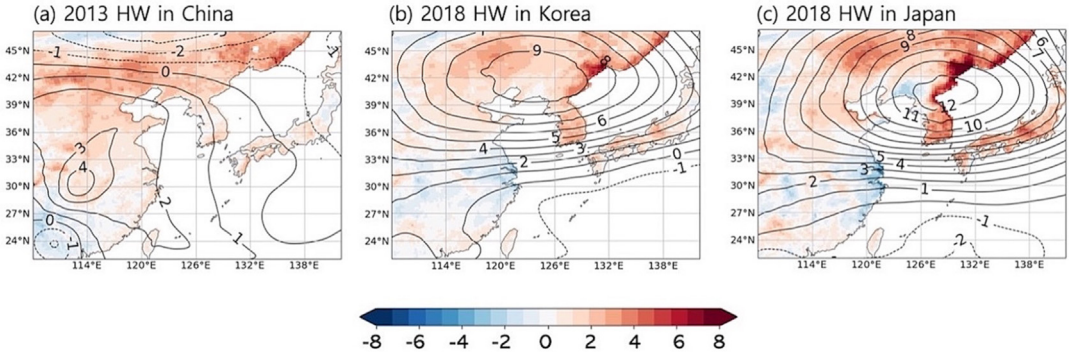

Fig. 5. Averaged pattern of 500 hPa geopotential height anomaly (black line contour) and 2-m air temperature anomaly, with color showing the singular CIR contribution (C_{CIR}) for the HW events over East Asia.

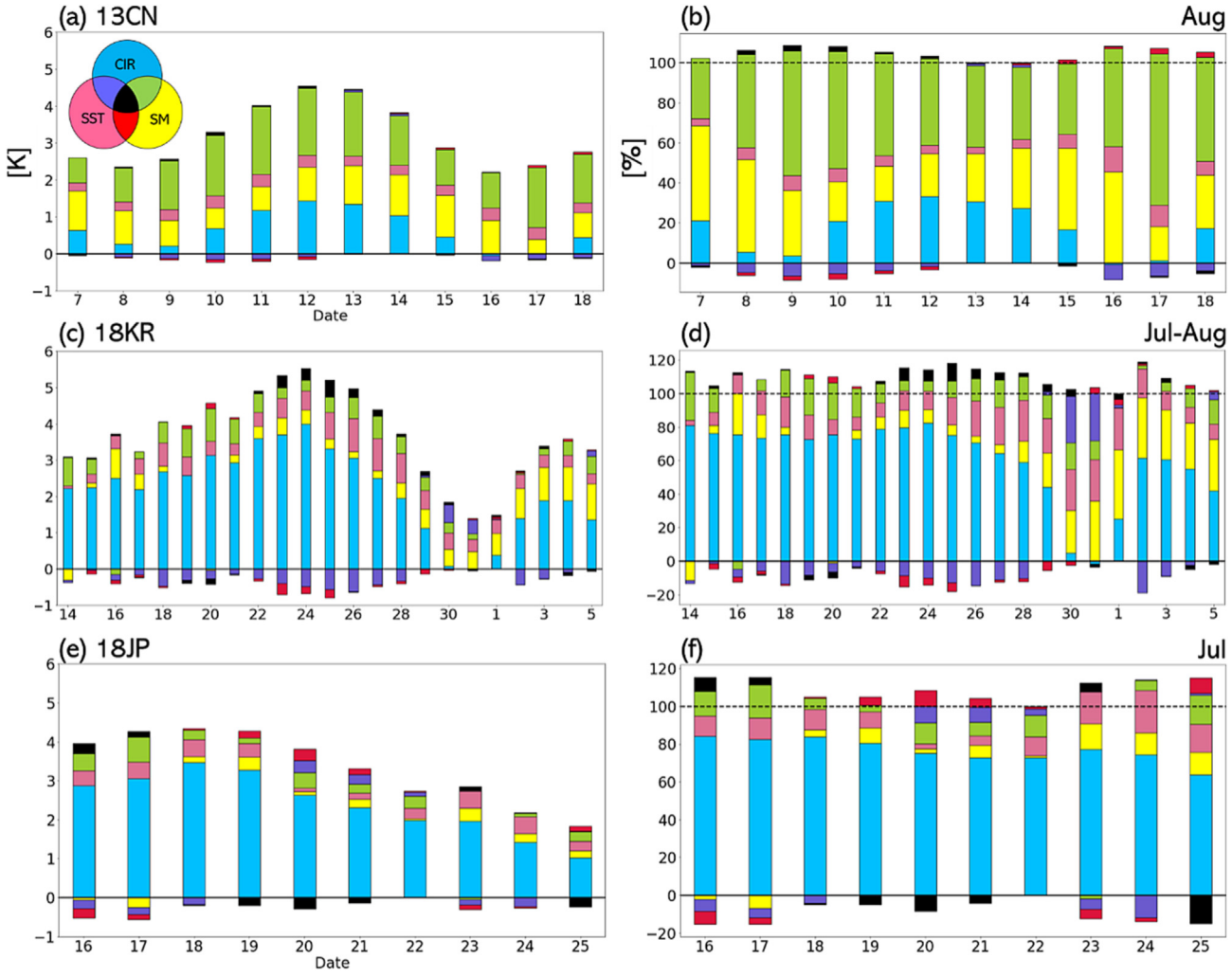

Fig. 6. Time series of physical driver contributions to absolute TX anomaly for HW cases in (a) China, (c) South Korea, and (e) Japan, with the relative contributions of each factor shown as percentages in (b), (d), and (f). Absolute contribution is calculated from 3-day moving average TX data and relative contribution is calculated by normalizing with total TX (ALL – CTL).

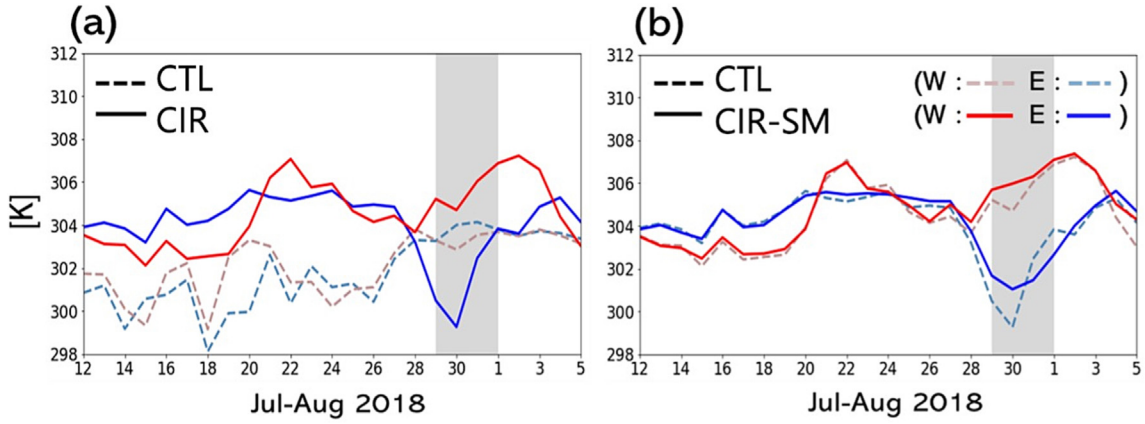

Fig. 7. Temporal changes in spatially averaged TX over the western (36°N–38°N, 126°E–128°E) and eastern (36°N–38°N, 128.5°E–129°E) regions of the Korean Peninsula divided by the Taebaek Mountains. (a) CIR impact (E_CIR) on TX differences over the windward (E) and leeward (W) areas in Korea, and (b) the influence of SST (E_CIR-SM) for the eastern and western region when pseudo-observational CIR is applied. The shaded periods show the period when the typhoon affected the Korean Peninsula.

the influence of the same high-pressure system during the 2018 Japanese HW period. There were also increases in incoming net shortwave radiation and thus sensible heat fluxes under the influence of this stagnant CIR (Supplementary Data, Fig. S2).

However, *EF* (i.e., relative contribution of direct heat into the atmosphere) did not show substantial changes despite the increases in surface shortwave radiation (Supplementary Data, Fig. S2), possibly because of ample rainfall and the related high

SM before the onset of the HW events (Fig. 3). This also explains why contributions of SM and its interaction with CIR to the Japanese HW were not as significant as for the Chinese and Korean HWs (Fig. 4). The same CIR pattern affected Korea and Japan, but the CIR contribution was relatively larger in Japan, with a decreased effect of the interaction between CIR with SM. Importantly, even after the direct passing of Typhoon Jongdari through Japan, the SM anomaly remained negative (Fig. 3). Heatwave intensity, however, decreased with the changes in CIR induced by the typhoon. This suggests that the CIR pattern plays an important role in HW occurrence and intensity, but that SM influences were negligible in HW generation in Japan (Fig. 6f). SST was the second most important factor in the 2018 Japanese HW, with a singular contribution of approximately 10%, similar to that of the 2018 Korean HW (Fig. 4). The contributions from interactions between other influential factors were relatively small compared to those in other regions.

4. Conclusions

This study conducted a factor separation analysis using the high-resolution regional atmospheric model, WRF to quantify contributions of key heatwave-controlling factors (i.e., large-scale circulation, SM, and SST) to recent heatwaves in East Asia: the 2013 Chinese HW, the 2018 South Korean HW, and the 2018 Japanese HW. To determine the contributions of the individual factors and their interactions to HW intensities, we constrained the factors in the model simulations using the corresponding climatology and pseudo-observations.

Our analysis showed significant spatial disparities in contribution of the heatwave-controlling factors across the East Asian region. Blockings of CIR, which caused strong surface radiative forcing and dry conditions, were persistent across the HW regions, but their contributions to HW intensity revealed regional differences in East Asia. During the 2013 Chinese HW event, SM and its interaction with the CIR mainly controlled HW intensity. The singular effect of CIR explained 20% of the TX anomaly in China. Meanwhile, CIR was a dominant factor in the 2018 Korean and Japanese HWs and exhibited no significant interactive impact with SM on HWs. SST was only a minor contributing factor to the Chinese HW, while it played a non-negligible role in the HW events in Korea and Japan. We speculate that dry conditions before the Chinese HW event increased the influence of SM, supporting that eastern China was a SM–temperature coupling hotspot, where evapotranspiration was strongly dependent on SM availability.

Temporal variations in contributions of the factors were apparent in all regions with different processes. Temporal changes in HW intensity were positively correlated with temporal changes in CIR contribution across the study regions. During the Chinese HW, HW intensity decreased with retreat of the high-pressure system owing to typhoon passages and subsequent reduction of surface shortwave radiation. The Korean and Japanese HW events also experienced reductions in HW intensities by typhoon. In the Japanese HW event, typhoon reduced the HW intensity and SM influence increased as soil dried out. However, despite change in the CIR by the typhoon during the Korean HW, HW intensity increased again with changes in wind direction from the warm ocean (i.e., large-scale warm advection by easterly winds) and sharp reduction of SM. This wind direction changes led to further temperature increases by the Foehn effect due to local warm easterly winds over the mountains located along the eastern coast of the Korean Peninsula. Our findings indicate that typhoons, typical summer events in East Asia, do not always alleviate HWs. Typhoons could prolong and reinforce HW event with the interaction with surface terrain and surrounding oceans, leading to changes in the contribution of CIR, SM, and SST interactions.

Furthermore, we found that the interaction of different factors tended to cancel each other in East Asia, but interactions contribute to intensifying HWs at specific times (e.g., during and after typhoon passages) and in specific regions (e.g., in China). The contribution of such interactions has not been considered in previous studies, and our findings suggest that singular factor effects may have been overestimated in previous studies because the synergistic effects were merged into the impacts of single factor contributions.

Despite the limitations of the factor separation analysis in elucidating causality, our analysis sheds light on understanding HW generation mechanisms in East Asia when the factor separation analysis is combined with the atmospheric mesoscale model and the physical interpretation of the model outputs. Our findings detail multifaceted perspectives to HW events, rather than simplifying them to a single variable such as soil moisture or the blocking of pressure systems in East Asia. Future work requires more attention to the interaction of driving factors and their role in the evolution of HWs, as well as their direct causal relationships.

Declaration of Competing Interest

The authors declare that they have no known competing financial interests or personal relationships that could have appeared to influence the work reported in this paper.

Acknowledgements

This research was supported by the Korea Meteorological Administration Research and Development Program (grant No. KMI2021-01610) and Korea Environment Industry & Technology Institute (KEITI) through Climate Change R&D Project for New Climate Regime Program, funded by Korea Ministry of Environment (MOE) (RS-2023-00221109).

Appendix A. Supplementary data

Supplementary data to this article can be found online at https://doi.org/10.1016/j.gsf.2023.101730.

References

Benson, D.O., Dirmeyer, P.A., 2021. Characterizing the relationship between temperature and soil extremes and their role in the exacerbation of heat waves over the contiguous United States. J. Clim. 34, 2175–2187.
Betts, A.K., Ball, J.H., Beljaars, A.C., Miller, M.J., Viterbo, P.A., 1996. The land surface-atmosphere interaction: A review based on observational and global modeling perspectives. J. Geophys. Res. Atmos. 101 (D3), 7209–7225.
Black, E., Blackburn, M., Harrison, G., Hoskins, B., Methven, J., 2004. Factors contributing to the summer 2003 European heatwave. Weather 59 (8), 217–223.
Cassou, C., Terray, L., Phillips, A.S., 2005. Tropical Atlantic influence on European heat waves. J. Clim. 18, 2805–2811.
Chen, R., Lu, R., 2015. Comparisons of the circulation anomalies associated with extreme heat in different regions of eastern China. J. Clim. 28, 5830–5844.
Choi, J., Song, C., Kim, E., Ahn J., 2022. Possible relationship between heatwaves in Korea and the summer blocking frequency in the Sea of Okhotsk. International J. Climatol. https://doi.org/10.1002/joc.7659.
Ding, T., Qian, W., Yan, Z., 2010. Changes in hot days and heat waves in China during 1961–2007. Int. J. Climatol. 30, 1452–1462. https://doi.org/10.1002/joc.1989.
Dole, R., Hoerling, M., Perlwitz, J., Eischeid, J., Pegion, P., Zhang, T., Quan, X.-W., Xu, T., Murray, D., 2011. Was there a basis for anticipating the 2010 Russian heat wave? Geophys. Res. Lett. 38, L06702. https://doi.org/10.1029/2010GL046582.
Dong, Z., Wang, L., Xu, P., Cao, J., Yang, R., 2023. Heatwaves similar to the unprecedented one in summer 2021 over western north America area projected to become more frequent in a warm world. Earth's Future 11, e2021EF003437.
Duchez, A., Frajka-Williams, E., Josey, S., Evans, D., Grist, J., Marsh, R., McCarthy, G., Sinha, B., Berry, D., Hirschi, J., 2016. Drivers of exceptionally cold North Atlantic

Ocean temperatures and their link to the 2015 European heat wave. Environ. Res. Lett. 11, 074004.
Fischer, E., Seneviratne, S.I., Lüthi, D., Schär, C., 2007. Contribution of land-atmosphere coupling to recent European summer heat waves. Geophys. Res. Lett. 34, L6707. https://doi.org/10.1029/2006GL02906.
Frölicher, T.L., Laufkötter, C., 2018. Emerging risks from marine heat waves. Nat. Commun. 9, 1–4.
Gómez, B., Charlton-Pérez, C., Lewis, H., Canday, B., 2020. The Met Office operational soil moisture analysis system. Remote Sens. 12, 3691.
Goyette, S., 2017. Numerical investigation with a coupled single-column lake-atmosphere model: using the Alpert-Stein factor separation methodology to assess the sensitivity of surface interactions. Clim. Dyn. 48, 2359–2373.
Ha, K.J., Yeo, J.H., Seo, Y.W., Chung, E.S., Moon, J.Y., Feng, X., Lee, Y.W., Ho, C.H., 2020. What caused the extraordinarily hot 2018 summer in Korea? J. Meteorol. Soc. Japan. Ser. II. 98, 153–167.
Hauser, M., Orth, R., Seneviratne, S.I., 2016. Role of soil moisture versus recent climate change for the 2010 heat wave in western Russia. Geophys. Res. Lett. 43, 2819–2826.
Hersbach, H., Bell, B., Berrisford, P., Hirahara, S., Horányi, A., Muñoz-Sabater, J., Nicolas, J., Peubey, C., Radu, R., Schepers, D., Simmons, A., Soci, C., Abdalla, S., Abellan, X., Balsamo, G., Bechtold, P., Biavati, G., Bidlot, J., Bonavita, M., De Chiara, G., Dahlgren, P., Dee, D., Diamantakis, M., Dragani, R., Flemming, J., Forbes, R., Fuentes, M., Geer, A., Haimberger, L., Healy, S., Hogan, R.J., Hólm, E., Janisková, M., Keeley, S., Laloyaux, P., Lopez, P., Lupu, C., Radnoti, G., de Rosnay, P., Rozum, I., Vamborg, F., Villaume, S., Thépaut, J.-N., 2020. The ERA5 global reanalysis. Q. J. R. Meteorol. Soc. 146, 1999–2049.
Hirschi, M., Seneviratne, S.I., Alexandrov, V., Boberg, F., Boroneant, C., Christensen, O.B., Formayer, H., Orlowsky, B., Stepanek, P., 2011. Observational evidence for soil-moisture impact on hot extremes in southeastern Europe. Nat. Geosci. 4, 17–21.
Hong, J.-W., Hong, J., Kwon, E., Yoon, D., 2019. Temporal dynamics of urban heat island correlated with the socio-economic development over the past half-century in Seoul, Korea. Environ. Pollut. 254, 112934. https://doi.org/10.1007/s10546-019-00452-5.
Iskandar, I., Lestari, D., Utari, P., Sari, Q., Setiabudidaya, D., Mardiansyah, W., 2018. How strong was the 2015/2016 El Niño event? J. Phys. Conf. Ser. 1011, 012030.
Jiang, J., Liu, Y., Mao, J., Wu, G., 2023. Extreme heatwave over Eastern China in summer 2022: the role of three oceans and local soil moisture feedback. Environ. Res. Lett. 18, 044025. https://doi.org/10.1088/1748-9326/acc5fb.
Jma, 2018. Characteristics and physical mechanisms on the record-breaking heavy rain and heatwave in 2018 July. Japan Meteorological Agency, pp. 21 https://www.jma.go.jp/jma/press/1808/10c/h30goukouon20180810.pdf.
Kawase, H., Imada, Y., Tsuguti, H., Nakaegawa, T., Seino, N., Murata, A., Takayabu, I., 2020. The heavy rain event of July 2018 in Japan enhanced by historical warming. Bull. Amer. Meteor. Soc. 101, S109-S114.
KMA, 2018. 2018 Abnormal Climate Report, Korea Meteorological Administration. Korea Meteorological Administration, 48 pp (in Korean).
Koster, R.D., Dirmeyer, P.A., Guo, Z., Bonan, G., Chan, E., Cox, P., Gordon, C.T., Kanae, S.J., Kowalczyk, E., Lawrence, D., Liu, P., Lu, C.-H., Malyshev, S., Mcavaney, B., Mitchell, K., Mocko, D., Oki, T., Oleson, K., Pitman, A., Sud, Y.C., Taylor, C.M., Verseghy, D., Vasic, R., Xue, Y., Yamada, T., 2004. Regions of strong coupling between soil moisture and precipitation. Science 305, 1138–1140.
Koster, R.D., Sud, Y.C., Guo, Z., Dirmeyer, P.A., Bonan, G., Oleson, K.W., Chan, E., Verseghy, D., Cox, P., Davies, H., Kowalczyk, E., Gordon, C.T., Kanae, S., Lawrence, D., Liu, P., Mocko, D., Lu, C.H., Mitchell, K., Malyshev, S., McAvaney, B., Oki, T., Yamada, T., Pitman, A., Taylor, C.M., Vasic, R., Xue, Y., 2006. GLACE: the global land–atmosphere coupling experiment. Part I: Overview. J. Hydrometeorol. 7, 590–610.
Lee, J., Hong, J., Noh, Y., Jiménez, P.A., 2020. Implementation of a roughness sublayer parameterization in the Weather Research and Forecasting model (WRF version 3.7. 1) and its evaluation for regional climate simulations. Geosci. Model Dev. 13, 521–536.
Li, J., Ding, T., Jia, X., Zhao, X., 2015. Analysis on the extreme heat wave over China around Yangtze River region in the summer of 2013 and its main contributing factors. Adv. Meteorol. 2015.
Lim, Y.J., Hong, J., Lee, T.Y., 2012. Spin-up behavior of soil moisture content over East Asia in a land surface model. Meteorol. Atmospheric Phys. 118, 151–161.
Lin, H., Mo, R., Vitart, F., 2022. The 2021 western north American heatwave and its subseasonal predictions. Geophys. Res. Lett. 49, e2021GL097036.
Liu, B., Zhu, C., Su, J., Ma, S., Xu, K., 2019. Record-breaking northward shift of the western North Pacific subtropical high in July 2018. J. Meteorol. Soc. Japan. Ser. II. 97 (4), 913–925.
Lorenz, R., Jaeger, E.B., Seneviratne, S.I., 2010. Persistence of heat waves and its link to soil moisture memory. Geophys. Res. Lett. 37, L09703. https://doi.org/10.1029/2010GL042.
Ma, H., Shao, H., Song, J., 2014. Modeling the relative roles of the foehn wind and urban expansion in the 2002 Beijing heat wave and possible mitigation by high reflective roofs. Meteorol. Atmospheric Phys. 123 (3), 105–114.
Meehl, G.A., Tebaldi, C., 2004. More intense, more frequent, and longer lasting heat waves in the 21st century. Science 305 (5686), 994–997.
Miralles, D.G., Teuling, A.J., Van Heerwaarden, C.C., De Arellano, J.V.G., 2014. Mega-heatwave temperatures due to combined soil desiccation and atmospheric heat accumulation. Nat. Geosci. 7 (5), 345–349.
Miralles, D.G., Gentine, P., Seneviratne, S.I., Teuling, A.J., 2019. Land–atmospheric feedbacks during droughts and heatwaves: state of the science and current challenges. Ann. N. Y. Acad. Sci. 1436 (1), 19–35.
Nakamura, H., Fukamachi, T., 2004. Evolution and dynamics of summertime blocking over the Far East and the associated surface Okhotsk high. Q. J. R. Meteorol. Soc. 130, 1213–1233.
Neal, E., Huang, C.S.Y., Nakamura, N., 2022. The 2021 Pacific northwest heat wave and associated blocking: Meteorology and the role of an upstream cyclone as a diabatic source of wave activity. Geophys. Res. Lett. 49, e2021GL097699.
Perkins, S.E., Alexander, L.V., Nairn, J.R., 2012. Increasing frequency, intensity and duration of observed global heatwaves and warm spells. Geophys. Res. Lett. 39, L20714. https://doi.org/10.1029/2012GL053361.
Petch, J.C., Short, C.J., Best, M.J., McCarthy, M., Lewis, H.W., Vosper, S.B., Weeks, M., 2020. Sensitivity of the 2018 UK summer heatwave to local sea temperatures and soil moisture. Atmospheric Sci. Lett. 21, e948.
Pfahl, S., Wernli, H., 2012. Quantifying the relevance of atmospheric blocking for co-located temperature extremes in the Northern Hemisphere on (sub-) daily time scales. Geophys. Res. Lett. 39, L12807. https://doi.org/10.1029/2012GL052261.
Ren, L., Zhou, T., Zhang, W., 2020. Attribution of the record-breaking heat event over Northeast Asia in summer 2018: the role of circulation. Environ. Res. Lett. 15, 054018.
Rousi, E., Kornhuber, K., Beobide-Arsuaga, G., Luo, F., Coumou, D., 2022. Accelerated western European heatwave trends linked to more-persistent double jets over Eurasia. Nat. Commun. 13, 3851.
Seneviratne, S.I., Lüthi, D., Litschi, M., Schär, C., 2006. Land–atmosphere coupling and climate change in Europe. Nature 443, 205–209.
Seneviratne, S.I., Corti, T., Davin, E.L., Hirschi, M., Jaeger, E.B., Lehner, I., Orlowsky, B., Teuling, A.J., 2010. Investigating soil moisture–climate interactions in a changing climate: A review. Earth-Sci. Rev. 99, 125–161.
Seneviratne, S.I., Wilhelm, M., Stanelle, T., van den Hurk, B., Hagemann, S., Berg, A., Cheruy, F., Higgins, M.E., Meier, A., Brovkin, V., Claussen, M., Ducharne, A., Dufresne, J.L., Findell, K.L., Ghattas, J., Lawrence, D.M., Malyshew, S., Rummukainen, M., Smith, B., 2013. Impact of soil moisture-climate feedbacks on CMIP5 projections: First results from the GLACE-CMIP5 experiment. Geophys. Res. Lett. 40, 5212–5217.
Seo, Y., Ha, K., 2022. Changes in land-atmosphere coupling increase compound drought and heatwaves over northern East Asia. NPJ Clim. Atmos. Sci. 5, 100. https://doi.org/10.1038/s41612-022-00325-8.
Shimpo, A., Takemura, K., Wakamatsu, S., Togawa, H., Mochizuki, Y., Takekawa, M., Tanaka, S., Ymashita, K., Maeda, S., Kurora, R., Murai, H., Kitabatake, N., Tsuguti, T., Mukougawa, H., Iwasaki, T., Kawamura, R., Kimoto, M., Takayabu, I., Takayabu, Y.N., Tanimoto, Y., Hirooka, T., Masumoto, Y., Watanabe, M., Tsuboki, K., Nakamura, H., 2019. Primary factors behind the heavy rain event of July 2018 and the subsequent heat wave in Japan. SOLA, 15A–003.
Song, I., Byun, U., Hong, J., Park, S., 2018. Domain-size and top-height dependence in regional predictions for East Asia in spring. Atmospheric Sci. Lett. 19, e799 https://doi:10.1002/asl.799.
Stein, U., Alpert, P., 1993. Factor separation in numerical simulations. J. Atmospheric Sci. 50, 2107–2115.
Sui, C.H., Chung, P.H., Li, T., 2007. Interannual and interdecadal variability of the summertime western North Pacific subtropical high. Geophys. Res. Lett. 34, 11701. https://doi.org/10.1029/2006GL029.
Teuling, A.J., Seneviratne, S.I., Stöckli, R., Reichstein, M., Moors, E., Ciais, P., Ciais, P., Luyssaert, S., van der Hurk, B., Ammann, C., Bernhofer, C., Dellwik, E., Gianelle, D., Gielen, B., Grunwald, T., Klumpp, K., Montagnani, L., Moureaux, C., Sottocornola, M., Wohlfahrt, G., 2010. Contrasting response of European forest and grassland energy exchange to heatwaves. Nat. Geosci. 3, 722–727.
van den Hurk, B., Doblas-Reyes, F., Balsamo, G., Koster, R.D., Senevitrane, S.I., Camargo, H., 2012. Soil moisture effects on seasonal temperature and precipitation forecast scores in Europe. Clim. Dyn. 38, 349–362.
van Garderen, L., Feser, F., Shepherd, T.G., 2021. A methodology for attributing the role of climate change in extreme events: a global spectrally nudged storyline. Nat. Hazards Earth Syst. Sci. 21, 171–186.
Wang, P., Tang, J., Wang, S., Dong, X., Fang, J., 2018. Regional heatwaves in China: A cluster analysis. Clim. Dyn. 50, 1901–1917.
Wehrli, K., Guillod, B.P., Hauser, M., Leclair, M., Seneviratne, S.I., 2018. Assessing the dynamic versus thermodynamic origin of climate model biases. Geophys. Res. Lett. 45, 8471–8479.
Wehrli, K., Guillod, B.P., Hauser, M., Leclair, M., Seneviratne, S.I., 2019. Identifying key driving processes of major recent heat waves. J. Geophys. Res. Atmos. 124, 11746–11765.
Wie, J., Moon, B.K., Hyun, Y.K., Lee, J., 2021. Impact of local atmospheric circulation and sea surface temperature of the East Sea (Sea of Japan) on heat waves over the Korean peninsula. Theor. Appl. Climatol. 144, 431–446.
Yeh, S., Won, Y., Hong, J., Lee, K., Kwon, M., Seo, K., Ham, Y., 2018. The record-breaking heat wave in 2016 over South Korea and its physical mechanism. Mon. Weather Rev. 146, 1463–1474. https://doi.org/10.1175/MWR-D-17-0205.1.
Yoon, D., Cha, D.H., Lee, G., Park, C., Lee, M.I., Min, K.H., 2018. Impacts of synoptic and local factors on heat wave events over southeastern region of Korea in 2015. J. Geophys. Res. Atmos. 123, 12–081.
Yoon, D., Cha, D.H., Lee, M.I., Min, K.H., Kim, J., Jun, S.Y., Choi, Y., 2020. Recent changes in heatwave characteristics over Korea. Clim. Dyn. 55, 1685–1696.

Yuan, W., Cai, W., Chen, Y., Liu, S., Dong, W., Zhang, H., Yu, G., Chen, Z., He, H., Guo, W., Liu, D., Liu, S., Xiang, W., Xie, Z., Zhao, Z., Liu, G., 2016. Severe summer heatwave and drought strongly reduced carbon uptake in Southern China. Sci. Rep. 6, 18813.

Yuan, X., Wang, L., Wood, E.F., 2018. Anthropogenic intensification of southern African flash droughts as exemplified by the 2015/16 season. Bull. Am. Meteorol. Soc. 99, S86–S90.

Zhang, J., Wu, L., Dong, W., 2011. Land-atmosphere coupling and summer climate variability over East Asia. J. Geophys. Res. Atmos. 116, D05117. https://doi.org/10.1029/2010JD014714.

Zscheischler, J., Seneviratne, S.I., 2017. Dependence of drivers affects risks associated with compound events. Sci. Adv. 3, e170026.